Ⅲ．研究成果の発表に関する一覧表

研究成果の刊行に関する一覧表

書籍

著者氏名	論文タイトル名	書籍全体の編集者名	書　籍　名	出版社名	出版地	出版年	ページ
鈴木　登	再発性多発軟骨炎	山口徹、北原光夫、福井次矢	今日の治療指針　私はこう治療している	医学書院	東京	2011	753-754

雑誌

発表者氏名	論文タイトル名	発表誌名	巻号	ページ	出版年
西根広樹、平本雄彦、木田博隆、松岡伸、峯下昌道、栗本典昭、宮澤輝臣	Assessing the site of maximal obstruction in the trachea using lateral pressure measurement during bronchoscopy.	Am J Respir Crit Care Med.	185 巻 1 号	23-33	2012
半田寛、峯下昌道、古屋直樹、木田博隆、西根広樹、井上健男、延山誠一、宮澤輝臣	中枢気道狭窄の評価における impulse oscillation system (IOS)の有用性の研究	聖マリアンナ医科大学雑誌	39 巻	113-121	2011
鈴木登	再発性多発性軟骨炎	膠原病ハンドブック（SSK 膠原　増刊）	通巻 3804 号	84-88	2011
鈴木登、遊道和雄、岡寛、山野嘉久	再発性多発性軟骨炎	リウマチ科	45(5)	510-514	2011
岡寛、山野嘉久、遊道和男、鈴木登、須賀万智	再発性多発軟骨炎の全国疫学調査	リウマチ科	44(3)	381-383	2010
鈴木登、尾崎承一、宮澤輝臣、肥塚泉、中島康雄、須賀万智、岡寛、山野嘉久、遊道和男	再発性多発性軟骨炎 (relapsing polychondritis) 診断・治療指針（案）2009 年度版	厚生労働科学研究費補助金　難治性疾患克服研究事業　再発性多発性軟骨炎の診断と治療体系の確立 平成 21 年度総括・分担研究報告書		38-47	2009
Sato T, Yamano Y, Ando H, Tomaru U, Shimizu Y, Okazaki T, Nagafuchi H, Shimizu J, Ozaki S, Miyazawa T, Yudoh K, Oka H, Suzuki N.	Serum level of soluble triggering receptor expressed on myeloid cells 1 (sTREM-1) as a biomarker of disease activity in relapsing polychondritis.	Clinical and Experimental Rheumatology	投稿中		
Oka H., Yamano Y., Shimizu J., Yudoh K., Suzuki N	Nationwide Epidemiologic Study of Relapsing Polychondritis in Japan; results of 239 cases.	Inflammatory and Regeneration	投稿中		

Ⅳ．研究成果の刊行物・別刷

炎）の出現に注意する．

再発性多発軟骨炎
relapsing polychondritis（RP）

鈴木　登　聖マリアンナ医科大学・難病治療研究センター長

病態と診断

再発性多発軟骨炎は，多彩な病態を呈する原因不明のまれな難治性炎症性疾患で，平均発症年齢は52.7歳，男女の罹患率はほぼ同等である．血中では軟骨組織構成成分に対する自己抗体や種々のケモカインの増加を認め，組織学的にも軟骨組織周囲への炎症細胞浸潤を認める．

初発症状として，約6割に耳介軟骨炎がみられ外耳介の疼痛・腫脹・発赤を認める．気道病変（気管軟骨炎，喉頭軟骨炎）はほぼ半数の患者に認め，咳嗽，喘鳴，呼吸困難を呈し予後を左右する．大動脈病変，動脈瘤，心臓弁膜症，腎障害，神経障害，骨髄異形成症候群や白血病，血管炎を合併する場合はそれぞれに対応が求められる．胸部の3D-CT検査は気道病変の検出に有用である．

診断には，①両側の耳介軟骨炎，②非びらん性多関節炎，③鼻軟骨炎，④結膜炎，強膜炎，ぶどう膜炎などの眼の炎症，⑤喉頭・気道軟骨炎，⑥感音性難聴，耳鳴り，めまいの蝸牛・前庭機能障害，の6項目のうち3項目以上を満たす，あるいは1項目以上陽性で，確定的な組織所見が得られる場合に診断される．臨床経過は約7割では治癒・改善するが，1割程度には死亡例もあり，呼吸不全と感染症が原因である．

治療指針

生命予後は改善しているものの，今でも致死的になりうる疾患であり，十分な治療を行い炎症の沈静化・軟骨破壊の防止に努める．経口ステロイドが治療の中心だが，気道病変をもつ場合には免疫抑制薬の使用を考慮する必要がある．軽症例や関節炎に対しては非ステロイド系抗炎症薬を用いる．難治性症例ではステロイドパルスを用いる．ステロイドや免疫抑制薬に抵抗性症例で生命予後に影響がある場合は生物学的製剤（レミケード，アクテムラ）が有効な場合がある（保険適用外，50-60%前後の奏効率）．

Ⓐ 内科的治療

1. **軽症例**　炎症が軽度で病変が耳介，鼻軟骨に病変が限局する場合は，以下の処方を行う．

℞ 処方例　下記1），2）のいずれかを用いる．

1）ロキソニン錠（60 mg）　3錠　分3　毎食後　保外　5

2）ハイペン錠（200 mg）　2錠　分2　朝・夕食後　保外

上記で不十分な場合は3）を用いる．

3）プレドニゾロン錠（5 mg）　2-4錠　分1-2　朝・夕食後　保外

2. **中等症例**　炎症が強く，気道病変，眼，心，腎臓などの臓器病変や血管炎合併例には以下の処方を行う．

℞ 処方例

プレドニゾロン錠（5 mg）　6-12錠（初期量）　分2-3　食後　初期量を2-4週継続し，以降1-2週ごとに10%程度減量　保外

3. **重症例**　炎症が非常に強く気道病変の進行や生命予後に影響がある場合には以下の処方を行う．

℞ 処方例

ソル・メドロール注　1回1,000 mg　1日1回　5%ブドウ糖500 mLに混和して2時間程度で点滴静注　3日間連続　保外

4. **ステロイド抵抗例**　ステロイドの減量で炎症が再燃する場合や，単独では効果が不十分な場合，免疫抑制薬を併用する．気道病変の進行がステロイド単剤ではコントロールしにくい場合には，早期からの免疫抑制薬の併用を考慮する．

℞ 処方例　下記の薬剤を症状に応じて適宜用いる．

1）リウマトレックスカプセル（2 mg）　2-4カプセル/週　分2　朝・夕食後　週に1-2日（2日の場合は連続した2日間）　保外　6

2）ネオーラルカプセル（50 mg）　2-4カプセル　分2　朝・夕食後　保外　55

3）エンドキサン錠（50 mg）　1-2錠　分1-2　朝・夕食後　保外

Ⓑ 外科的治療・その他の治療

気道病変に対しては，気管切開術，気管・気管支狭窄例にはステント（expandable metallic stent）挿入や，気管形成術，末梢気道病変の虚脱を防ぐため二相式気道陽圧療法を施行する．心血管病変には外科的手術が必要になる．

患者説明のポイント

- 十分な治療を行い，炎症をコントロールすることにより近年は予後が改善してきている．
- 局所症状は長期にわたり寛解と再燃を繰り返し，その経過の中で多彩な症状が出現する可能性がある．
- 現病と治療薬により易感染状態にあるため，感染予防に留意する．

・炎症部の軟骨は脆弱化しているので，圧迫などで変形が助長されるため，局所の安静を保つ．

線維筋痛症と慢性疲労症候群

fibromyalgia (FM) and chronic fatigue syndrome (CFS)

松本美富士　藤田保健衛生大学教授・内科（七栗サナトリウム）

病態と診断

Ⓐ 病態

線維筋痛症（FM）および慢性疲労症候群（CFS）ともに原因不明のリウマチ病態であり，多彩な身体，神経・精神症状を呈するが，他覚所見に乏しく，機能性身体疾患群（functional somatic syndrome：FSS）に分類される疾患である．両疾患はFSSの特徴である相互の類似性，合併しやすさ，治療の共通性などがある．身体の広範な部位の慢性疼痛，あるいは慢性の激しい疲労のいずれが主症状であるかによってFM，CFSと分類される．

Ⓑ 診断

いずれも特異的所見がないため，除外診断的要素が強い．種々の疾患が鑑別診断の対象となるが，これら疾患の基本病像や特徴的臨床所見・検査所見から，その疾患概念の認識があれば鑑別は比較的容易である．

1. FM　米国リウマチ学会（1990年）分類基準が国際的に用いられており，本邦例での有用性も検証されている．3か月以上にわたる身体の広範な部位の疼痛と解剖学的に定義化された身体の18か所のうち，11か所以上に圧痛が存在すればFMと診断される．FMのみで発症するものとリウマチ性疾患など既存の疾患に併発するものとがある．

2. CFS　日本疲労学会のCFS診断指針（2008年）が作成され，既存の疾患では説明できない激しい疲労・倦怠感が6か月以上存在し，多彩な身体，神経・精神症状と微熱，リンパ節腫脹，非滲出性咽頭炎などが認められればCFSと診断される．

治療方針

何よりも重要のことは本疾患の存在を医療側が認識して診療にあたることと，患者・周囲への疾患受容への教育である．多彩な症状を呈することから，過剰な検査の実施，対症療法の多量の薬物療法，過度の安静を指示しがちであるが，これらは有害である．FMでは「線維筋痛症診療ガイドライン2009」が作成されている．

原因不明のため根治療法はなく，治療の基本は症状の緩和である．EBM的に有効性が確認されているのは，FMでは抗うつ薬，抗けいれん薬，認知行動療法（CBT）と有酸素運動療法であり，CFSでもCBT，有酸素運動療法が有効である．エビデンスはないが漢方製剤を用いることもある．疼痛に対して非ステロイド系抗炎症薬，麻薬性鎮痛薬は無効である．また，精神医学的側面が強い症例は精神科医・心療内科医の介入が必要である．

Ⓐ 薬物療法

1. 疲労・倦怠感に対して

℞ 処方例　下記のいずれか，または適宜組み合わせて用いる．

1) ハイシー顆粒（25%）　3-4g（製剤量として）　分3　毎食後 (保外)
2) ノイキノン錠（10mg）　3錠　分3　毎食後 (保外)
3) メチコバール錠（500μg）　3錠　分3　毎食後 (保外)

いずれも効果不十分なら適宜1.5倍量まで増量し，分服する．

2. うつ症状，不安症状，睡眠障害に対して

℞ 処方例　下記のいずれかを用いるか，適宜組み合わせて用いる．

1) トレドミン錠（25mg）　1錠　分1　就寝前　副作用がなければ適宜2-3錠/日に増量，分服 [11]
2) トリプタノール錠（10mg）　1錠　分1　就寝前　副作用がなければ適宜2-3錠/日に増量，分服 [12]
3) ワイパックス錠（0.5mg）　2錠　分2　朝・夕食後　効果が十分でなければ，適宜3-4錠/日に増量，分服 [8]
4) レンドルミン錠（0.25mg）　1錠　分1　就寝前

3. 疼痛に対して

℞ 処方例　下記のいずれかを用いるか，適宜組み合わせて用いる．抗うつ薬との併用も行う．

1) ノイロトロピン錠（4単位）　4錠　分2　朝・夕食後 (保外)　適宜6-8錠/日に増量，分服
2) ノイロトロピン注（3.6単位）　1回1-2アンプル　1日1回　静注 (保外)
3) ガバペン錠（400mg）[15]　2錠　分2　朝・夕食後 (保外)　適宜3-6錠/日に増量，分服，またはリリカカプセル（75mg）　2カプセル　分2　朝・夕食後 (保外)　適宜4-6カプセル/日に増量，分服

疼痛が激しい場合は，トラマール注（100mg）の筋注（必要に応じて4-5時間ごとに反復）が有

Assessing the Site of Maximal Obstruction in the Trachea Using Lateral Pressure Measurement during Bronchoscopy

Hiroki Nishine[1], Takehiko Hiramoto[1], Hirotaka Kida[1], Shin Matsuoka[2], Masamichi Mineshita[1], Noriaki Kurimoto[3], and Teruomi Miyazawa[1]

[1]Division of Respiratory and Infectious Diseases, Department of Internal Medicine, [2]Department of Radiology, and [3]Division of Chest Surgery, Department of Surgery, St. Marianna University School of Medicine, Kawasaki, Japan

Rationale: Lateral airway pressure can provide valuable physiological information during bronchoscopy.
Objectives: To evaluate tracheal obstruction during intervention.
Methods: To prospectively measure lateral airway pressure during bronchoscopy using a double-lumen catheter in 15 healthy subjects and 30 patients with tracheal obstruction. Pressure difference was used to evaluate the site of maximal obstruction. The angle between pressure recordings on either side of the stenosis was measured simultaneously (pressure–pressure curves) to assess the degree of tracheal obstruction.
Measurements and Main Results: In the experimental study, the angle of the pressure–pressure curve was unaffected by breathing maneuvers whereas the pressure difference was affected. In healthy subjects, no pressure difference between the carina and trachea was observed during tidal breathing, and the angle was close to 45°. In patients with tracheal obstruction, the dyspnea scale, pressure difference, and angle changed significantly beyond 50% obstruction ($P < 0.0001$). After stenting, the pressure difference disappeared and the angle was close to 45°. The degree of tracheal obstruction was significantly correlated with the pressure difference ($r = 0.83$, $P < 0.0001$) and angle ($r = -0.84$, $P < 0.0001$). The cross-sectional area, dyspnea scale, pulmonary function tests, pressure difference, and the angle significantly improved after procedures ($P < 0.0001$). Responder rates on the modified Medical Research Council Scale were 84.6% for obstructions above 80%, and 58.8% for obstructions between 50 and 80%.
Conclusions: The direct measurement of pressure difference and the angle of the pressure–pressure curve represent a new assessment modality for the success of interventional bronchoscopy. Measuring lateral airway pressure could estimate the need for additional procedures better than bronchoscopy alone.
Public trial registered at umin.ac.jp (UMIN000002400).

Keywords: angle of pressure–pressure curve; dyspnea scale; pressure difference; site of maximal obstruction; stenting

AT A GLANCE COMMENTARY

Scientific Knowledge on the Subject

In interventional bronchoscopy the location of the flow-limiting segment is assessed by evaluating the flow–volume curve. However, to date, there is no quantitative examination for assessing the results of interventional bronchoscopy in real time.

What This Study Adds to the Field

By measuring lateral airway pressure on each side of the stenosis and plotting the two pressures (pressure–pressure curves) during quiet breathing, the site of maximal obstruction and the degree of stenosis can be determined quantitatively. The results suggest that the pressure difference and the angle of the pressure–pressure curve may be used to estimate the outcome of interventional bronchoscopy.

In patients with severe malignant airway stenosis, interventional bronchoscopy is considered to be a method for maintaining airway patency (1). Patients referred for treatment of airway stenosis are typically asymptomatic until critical narrowing of the airway occurs. The degree of dyspnea depends on the degree of airway obstruction and becomes severe when well over 70% of the tracheal lumen is obstructed (2). In our previous studies, placement of the stent at the flow-limiting segment (FLS) provided the greatest functional benefit to patients with central airway stenosis (3, 4).

Dynamic airway compression causes the formation of an FLS in the central airways during forced expiration. With the use of airway catheters in dogs (5–7) and in human subjects (8–10), the FLS could be located by measuring lateral airway pressure (P_{lat}) during induced flow limitation generated by either an increase in pleural pressure or a decrease in downstream pressure.

Analysis of the flow–volume curve can be used to define the nature of the stenosis and to provide reliable information on the efficacy of stenting (4, 11–15). However, flow–volume curves cannot identify the precise location of the lesion where airway resistance increases, nor can it immediately define the outcome of stenting. Because assessment of the FLS requires forced expiratory vital capacity maneuvers, detecting flow limitation by measuring P_{lat} cannot be performed during bronchoscopy. We therefore proposed a simple and well-tolerated bronchoscope-guided technique using P_{lat} measurements to locate the site of maximal obstruction and to estimate the outcome of intervention.

The theory behind the measurement of P_{lat} is as follows. A double-lumen airway catheter capable of simultaneously measuring P_{lat} at two sites in the trachea can be used to assess tracheal obstruction. If the catheter is positioned so that the two holes are located on each side of a stenosis, then the two pressures plotted against each other (pressure–pressure [P–P] curve) will display a line with a slope less than 45° due to

(Received in original form April 19, 2011; accepted in final form September 29, 2011)

Supported by the Japan Society for the Promotion of Science and by Grants-in-Aid for Scientific Research (20590908).

Author Contributions: H.N. and T.M., study concept and design; T.H., acquisition of data; H.K. and S.M., analysis and interpretation of data; M.M., H.N., and N.K., preparation of manuscript. T.M. had complete access to all data in this study and takes full responsibility for its integrity and for the accuracy of data analysis.

Correspondence and requests for reprints should be addressed to Teruomi Miyazawa, M.D., Ph.D., St. Marianna University School of Medicine, 2-16-1 Sugao Miyamae-ku, Kawasaki, 216-8511 Japan. E-mail: miyazawat@marianna-u.ac.jp

Am J Respir Crit Care Med Vol 185, Iss. 1, pp 24–33, Jan 1, 2012

Originally Published in Press as DOI: 10.1164/rccm.201104-0701OC on October 13, 2011
Internet address: www.atsjournals.org

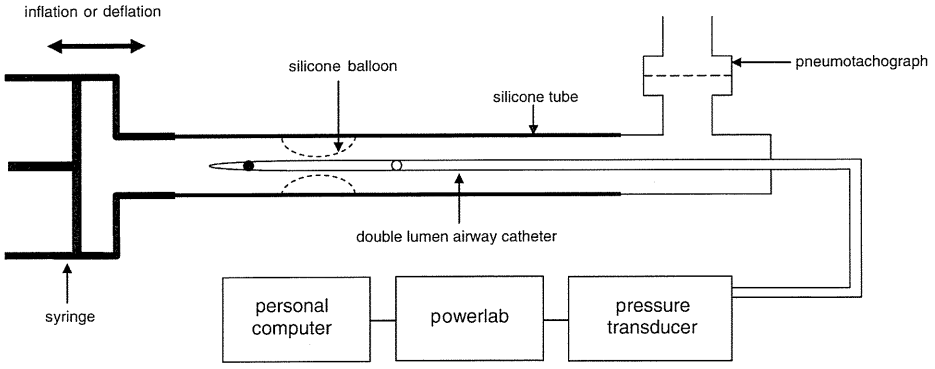

Figure 1. Experimental model of tracheal stenosis. When the silicone tube was partially or completely obstructed by the balloon in the lumen, lateral pressure was measured simultaneously at *white* and *black points*. The catheter was connected to two identical pressure transducers and pressure was recorded on an instrumentation amplifier device.

resistance between the two points. If the two holes are located downstream or upstream from the stenosis, pressure between these sites will be in phase and if plotted against each other, will display a straight line with a slope of 45°.

The aim of this study is to assess the efficacy and feasibility of measuring P_{lat} simultaneously at two points to determine the site of maximal obstruction. To validate this method, we first built an experimental model to simulate a tracheal obstruction and to assess the characteristics of central airway mechanics, regardless of the type of breathing maneuver employed. Then, to test the clinical feasibility, we assessed P_{lat} and P–P curves in patients with tracheal obstruction during intervention. Some of these results have been previously reported in the form of abstracts (16, 17).

METHODS

Experimental Model Validation

A silicone tube was placed horizontally and could be partially or completely obstructed by inserting a silicone balloon into the lumen and inflating with a plastic syringe (Figure 1). The silicone tube was exposed to positive and negative driving pressure by inflating and deflating 100 ml regularly to emulate a regular respiratory cycle. Lateral airway pressure (P_{lat}) was measured at two points during changes in the respiratory rate, flow, and volume. Flow was measured with a pneumotachograph (Lilly type; Chest Corp., Tokyo, Japan) on one side of the tube.

Clinical Feasibility

Between August 2007 and July 2010, we performed a prospective study that was approved by the Research Ethics Committee at St. Marianna University School of Medicine (Kawasaki, Japan). Thirty patients with tracheal obstruction underwent P_{lat} measurement after meeting the following criteria: patients scored grade 2 or more on the modified Medical Research Council (MMRC) Scale and had a minimum of 50% obstruction on multidetector computed tomography (MDCT). We also investigated 15 healthy subjects.

MDCT was performed with a 64-detector row CT scanner (Aquilion-64; Toshiba Medical, Tokyo, Japan) as previously described (18, 19). The degree of tracheal obstruction was defined as $(CSA_{normal} - CSA_{actual})/CSA_{normal}$ (CSA, cross-sectional area). Variable stenosis was defined as an additional narrowing of more than 50% of the CSA during expiration (20–22), and an additional narrowing of less than 50% during expiration suggested a fixed stenosis.

Lateral Airway Pressure Measurement

All patients were anesthetized by intravenous injection of propofol. After intubation with a rigid bronchoscope (EFER, La Ciotat, France), a double-lumen airway catheter (Fuji Systems, Tokyo, Japan) was inserted into the trachea during bronchoscopy. The catheter is constructed of nylon elastomer with two holes premanufactured into the side at 5-cm intervals, with an outer diameter of 1.7 mm. The catheter was connected to two identical pressure transducers (SCX01DN; Sensortechnics, Munich, Germany). P_{lat} was measured simultaneously at two points during spontaneous breathing with light general anesthesia before and after intervention. The site of maximal obstruction was evaluated on the basis of the pressure difference between the proximal and distal sites of the stenosis. P_{lat} at the two points was plotted on an oscilloscope (pressure–pressure [P–P] curve). The angle of the P–P curve was defined as the angle between the peak inspiratory and expiratory pressure points and the baseline of the angle.

Statistical Analysis

All analyses were performed with SAS software (release 8.2; SAS Institute, Cary, NC). Correlations among pressure difference, the angle of the P–P curve, and the CSA were evaluated using the Spearman correlation coefficient. Responders were defined as any patient with an increase in FVC or FEV_1 exceeding 200 ml and 12% of the baseline value by pulmonary function test. Any patient with an improvement in MMRC Scale of two or more grades was considered to be a clinical responder. A receiver operating characteristic curve was used to evaluate the usefulness of the pressure difference and the angle of the P–P curves.

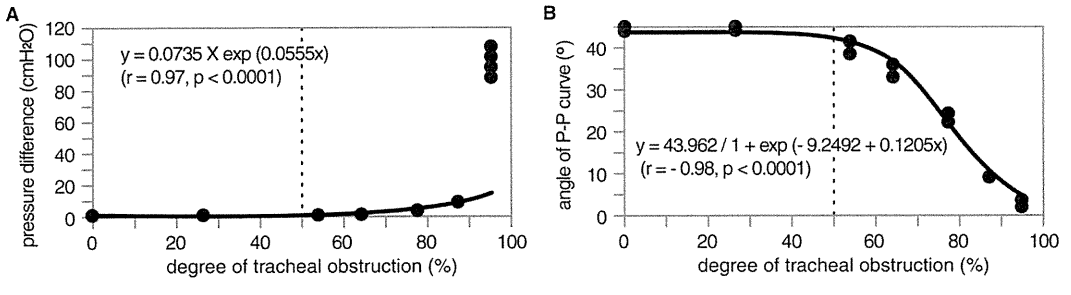

Figure 2. Correlations among pressure difference, angle of pressure–pressure (P–P) curve, and degree of tracheal obstruction for the experimental model. *Dotted line* shows the threshold for 50% tracheal obstruction. (*A*) The pressure difference and (*B*) the angle of the P–P curves are significantly correlated with the degree of tracheal obstruction ($r = 0.97$, $P < 0.0001$ and $r = -0.98$, $P < 0.0001$, respectively). (*A*) The pressure difference increased above 50% obstruction. When the degree of obstruction decreased, the angle of the P–P curve increased toward 45°. (*B*) However, when the degree of obstruction was greater, the angle of the P–P curve was close to 0°.

TABLE 1. VARIATION OF PRESSURE DIFFERENCE (CHANGING RESPIRATORY RATE, FLOW, AND VOLUME) IN THE EXPERIMENTAL MODEL

	Respiratory Rate (*breaths/min*)			*P* Value for
Degree of Obstruction (%)	10	20	30	Degree of Obstruction
0.0 ± 4.8	0.03 ± 0.01	0.02 ± 0.01	0.03 ± 0.01	
26.5 ± 2.0	0.02 ± 0.01	0.03 ± 0.00	0.02 ± 0.01	
54.0 ± 1.9	0.23 ± 0.01	0.24 ± 0.02	0.26 ± 0.02	
64.2 ± 0.4	0.47 ± 0.03	0.59 ± 0.06	0.51 ± 0.08	<0.0001
77.5 ± 0.7	1.47 ± 0.11	1.74 ± 0.11	1.92 ± 0.11	
87.2 ± 0.7	5.65 ± 0.80	6.49 ± 0.65	6.63 ± 0.41	
95.1 ± 0.1	15.39 ± 1.13	14.83 ± 0.22	14.15 ± 0.79	
P value for respiratory rate		0.6716		0.0001*
	Airflow (*L/s*)			*P* Value for
Degree of Obstruction (%)	1.0	1.5	2.0	Degree of Obstruction
0.0 ± 4.8	0.14 ± 0.02	0.22 ± 0.07	0.59 ± 0.09	
26.5 ± 2.0	0.16 ± 0.02	0.24 ± 0.02	0.49 ± 0.09	
54.0 ± 1.9	0.32 ± 0.04	0.63 ± 0.13	0.98 ± 0.14	
64.2 ± 0.4	0.55 ± 0.07	0.89 ± 0.09	1.47 ± 0.13	<0.0001
77.5 ± 0.7	1.79 ± 0.22	2.79 ± 0.21	3.88 ± 0.25	
87.2 ± 0.7	5.72 ± 0.47	8.71 ± 0.55	15.86 ± 0.63	
95.1 ± 0.1	45.78 ± 2.93	96.29 ± 8.58	152.87 ± 9.72	
P value for airflow		<0.0001		<0.0001*
	Volume (*ml*)			*P* Value for
Degree of Obstruction (%)	50	100	150	Degree of Obstruction
0.0 ± 4.8	0.03 ± 0.0.01	0.11 ± 0.02	0.21 ± 0.02	
26.5 ± 2.0	0.04 ± 0.01	0.12 ± 0.01	0.24 ± 0.02	
54.0 ± 1.9	0.07 ± 0.01	0.22 ± 0.01	0.42 ± 0.08	
64.2 ± 0.4	0.12 ± 0.01	0.39 ± 0.03	0.73 ± 0.10	<0.0001
77.5 ± 0.7	0.29 ± 0.03	0.87 ± 0.08	1.73 ± 0.07	
87.2 ± 0.7	0.52 ± 0.03	1.82 ± 0.12	3.46 ± 0.37	
95.1 ± 0.1	3.41 ± 0.42	10.80 ± 1.14	34.42 ± 1.21	
P value for volume		<0.0001		<0.0001*

Differences were assessed by two-way analysis of variance. Values are represented as means ± standard deviation.
* *P* for interaction.

RESULTS

Experimental Model Validation

The degree of tracheal obstruction was significantly correlated with the pressure difference ($r = 0.97$, $P < 0.0001$) and the angle of the pressure–pressure (P–P) curve ($r = -0.98$, $P < 0.0001$) (Figure 2). When lateral airway pressure (P_{lat}) was measured during changes in the respiratory rate (10, 20, and 30/min), flow (1.0, 1.5, and 2.0 L/s), and volume (50, 100, and 150 ml), there was no significant difference between the pressure difference and respiratory rate ($P = 0.6716$). However, statistically significant differences were seen in the pressure difference for changes in flow ($P < 0.0001$) and volume ($P < 0.0001$) (Table 1). There was no significant difference between the angle of P–P curves and the type of breathing maneuver employed, such as respiratory rate ($P = 0.8986$), flow ($P = 0.9978$), and volume ($P = 0.9995$). Statistically significant differences in the angle of the P–P curves for changes in the degree of tracheal obstruction were recognized ($P < 0.0001$) (Table 2).

Clinical Feasibility

Measurements for P_{lat} were taken in 15 healthy subjects and 30 patients with tracheal obstruction (Table 3). P_{lat} measurement required an additional 5 minutes of procedure time and no adverse events were noted as a result of this bronchoscopic approach.

In healthy subjects, there were no flow limitations (Table 3) or pressure differences between the carina and upper trachea (0.10 ± 0.22 cm H_2O) during tidal breathing (Figure 3A). The P–P curves were linear and the angle of the P–P curves was close to 45° (44.6 ± 0.9°) (Figure 3B).

Characteristics of patients with tracheal obstruction are shown in Table 4. In all patients, clinical assessment, endoscopic examination, and pulmonary function before and immediately after interventional bronchoscopy showed improvements. Pulmonary function tests could not be performed on patients with poor performance status (n = 2) and after tracheostomy (n = 2). In pulmonary function tests, FVC, FEV_1, and PEF increased significantly after procedures ($P = 0.044$, $P < 0.0001$, and $P < 0.0001$, respectively) (Table 5). MMRC Scale scores improved after procedures ($P < 0.0001$) (Table 5). Significant improvements for all patients were observed in the degree of tracheal obstruction ($P < 0.0001$), the pressure difference ($P < 0.0001$), and the angle of the P–P curve ($P < 0.0001$) (Table 5). The proportion of responders to treatment was 70.0% for the modified Medical Research Council (MMRC) Scale, 50.0% for FVC, and 80.8% for FEV_1 (Table 5).

Correlations between the pressure difference and the degree of tracheal obstruction and between the angle of the P–P curve and the degree of tracheal obstruction are shown in Figure 4. We found that the degree of tracheal obstruction was significantly correlated with the pressure difference ($r = 0.83$, $P < 0.0001$) and the angle of the P–P curve ($r = -0.84$, $P < 0.0001$). Pressure differences increased significantly above 50% obstruction and increased dramatically above 70% obstruction (Figure 4A). If the cross-sectional area (CSA) was small, the angle of the P–P curve was close to 0°. However, after interventional bronchoscopy, the CSA increased and the angle of the P–P curve

TABLE 2. VARIATION OF ANGLE OF PRESSURE–PRESSURE CURVES (CHANGING RESPIRATORY RATE, FLOW, AND VOLUME) IN THE EXPERIMENTAL MODEL

	Respiratory Rate (*breaths/min*)			*P* Value for
Degree of Obstruction (%)	10	20	30	Degree of Obstruction
0.0 ± 4.8	40.3 ± 1.4	41.3 ± 1.9	39.7 ± 1.4	
26.5 ± 2.0	40.2 ± 2.0	40.1 ± 2.1	39.1 ± 1.1	
54.0 ± 1.9	40.3 ± 0.4	40.3 ± 0.8	40.2 ± 0.7	
64.2 ± 0.4	36.6 ± 1.1	36.1 ± 1.0	36.6 ± 1.2	<0.0001
77.5 ± 0.7	25.9 ± 2.2	26.3 ± 2.0	26.5 ± 1.7	
87.2 ± 0.7	12.9 ± 1.6	12.9 ± 1.6	13.4 ± 1.0	
95.1 ± 0.1	4.3 ± 0.9	4.1 ± 0.8	3.9 ± 0.9	
P value for respiratory rate		0.8986		0.9124*
	Airflow (L/sec)			*P* Value for
Degree of Obstruction (%)	1.0	1.5	2.0	Degree of Obstruction
0.0 ± 4.8	41.7 ± 0.6	42.0 ± 0.6	42.1 ± 0.9	
26.5 ± 2.0	42.8 ± 0.6	42.5 ± 0.7	42.4 ± 0.4	
54.0 ± 1.9	40.3 ± 0.7	40.0 ± 0.3	40.3 ± 0.7	
64.2 ± 0.4	36.2 ± 1.0	36.2 ± 0.8	35.9 ± 1.2	<0.0001
77.5 ± 0.7	25.5 ± 1.3	25.6 ± 1.1	25.7 ± 0.7	
87.2 ± 0.7	12.1 ± 0.8	11.0 ± 0.3	10.8 ± 0.7	
95.1 ± 0.1	1.4 ± 0.3	1.1 ± 0.2	1.2 ± 0.5	
P value for airflow		0.9978		0.9764*
	Volume (*ml*)			*P* Value for
Degree of Obstruction (%)	50	100	150	Degree of Obstruction
0.0 ± 4.8	43.9 ± 0.5	43.6 ± 0.7	43.3 ± 0.4	
26.5 ± 2.0	42.0 ± 1.0	42.4 ± 0.6	42.1 ± 0.4	
54.0 ± 1.9	40.8 ± 0.5	40.4 ± 0.7	40.5 ± 0.3	
64.2 ± 0.4	38.8 ± 0.5	38.5 ± 0.9	38.8 ± 0.9	<0.001
77.5 ± 0.7	32.2 ± 0.5	32.2 ± 1.3	31.8 ± 1.0	
87.2 ± 0.7	23.7 ± 0.9	23.1 ± 1.3	22.9 ± 1.2	
95.1 ± 0.1	6.3 ± 0.6	5.3 ± 0.3	4.5 ± 1.3	
P value for volume		0.9995		0.9487*

Differences were assessed by two-way analysis of variance. Values are represented as means ± standard deviation.
* *P* for interaction.

was close to 45° (Figure 4B). Receiver operating characteristic analysis indicated that the optimal cutoff point for pressure difference and the angle of P–P curves was 50% for tracheal obstruction, with 85.7 and 86.1% sensitivity and 73.9 and 79.2% specificity, respectively.

The MMRC Scale was significantly correlated with the degree of tracheal obstruction ($r = 0.76$, $P < 0.0001$), the pressure difference ($r = -0.65$, $P < 0.0001$), the angle of the P–P curve ($r = -0.68$, $P < 0.0001$), FEV_1 ($r = -0.54$, $P < 0.0001$), and PEF ($r = -0.72$, $P < 0.0001$), but there was no significant correlation between the MMRC Scale and FVC ($r = -0.09$, $P = 0.508$) before and after intervention. Dyspnea significantly increased when the airway lumen was obstructed by more than 50% ($P < 0.0001$). The mean degree of tracheal obstruction for each MMRC grade was as follows: 40.0% for grade 0, 55.9% for grade 1, 68.4% for grade 2, 71.4% for grade 3, and 80.1% for grade 4 (P for trend < 0.0001). The relation between the baseline of the degree of tracheal obstruction and the change in MMRC (ΔMMRC) is shown in Table 6. The clinical responder rate was 84.6% for obstructions above 80% and 58.8% for obstructions between 50 and 80%.

The pressure difference was significantly correlated with FEV_1 ($r = -0.45$, $P < 0.0001$) and PEF ($r = -0.62$, $P < 0.0001$); however, there was no significant correlation between the pressure difference and FVC ($r = -0.14$, $P = 0.252$) (Table 7). The angle of the P–P curve was significantly correlated with FEV_1 ($r = -0.44$, $P = 0.0001$) and PEF ($r = -0.53$, $P < 0.0001$), whereas there was no significant correlation between the angle of the P–P curve and FVC ($r = -0.09$, $P = 0.443$) (Table 7).

Of the 30 patients with tracheal obstruction, 18 were fixed stenoses and 12 were variable stenoses. For patients with fixed stenosis, the P–P curve was linear and no significant change was observed in the angle of the P–P curve between inspiratory and

TABLE 3. DEMOGRAPHICS AND PULMONARY BASELINE OF HEALTHY SUBJECTS AND PATIENTS WITH TRACHEAL OBSTRUCTION

	Healthy Subjects (*n = 15*)	Tracheal Obstruction (*n = 30*)
Age, yr		
Mean ± SD	63.3 ± 13.4	59.6 ± 13.5
Range	26–84	35–81
Sex		
Male	10	21
Female	5	9
Height, cm	159.3 ± 10.0	161.2 ± 8.6
Body weight, kg	54.1 ± 10.5	52.4 ± 12.8
VC, L	3.1 ± 0.8	2.7 ± 1.0
VC, % predicted	103.3 ± 13.6	83.3 ± 23.8*
FVC, L	3.1 ± 0.8	2.6 ± 1.1
FEV_1, L	2.4 ± 0.6	1.2 ± 0.5†
FEV_1, % predicted	101.5 ± 14.4	48.7 ± 19.3†
FEV_1/FVC, %	75.7 ± 8.9	48.1 ± 19.6†
PEF, L/s	7.3 ± 1.9	2.1 ± 0.8†

Comparisons between control subjects and patients were performed by unpaired *t* tests for quantitative variables and Fisher exact tests for categorical variables.
Values are represented as means ± standard deviation.
* $P < 0.01$.
† $P < 0.0001$.

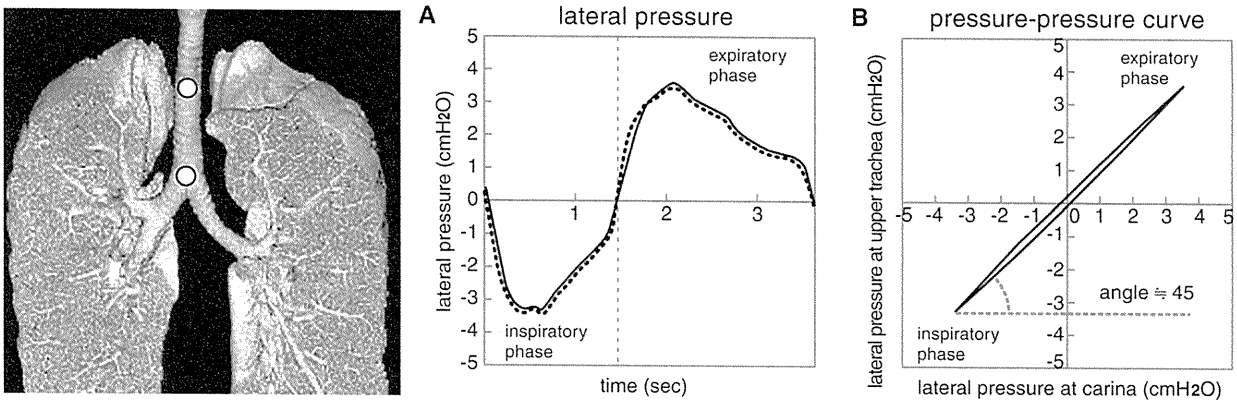

Figure 3. Typical patterns of lateral airway pressure (P_{lat}) measurements during tidal breathing in a healthy subject. P_{lat} is measured simultaneously at the *white points* (upper trachea and carina). (*A*) There are no pressure differences between the carina and upper trachea (*black line,* carina; *dotted line,* upper trachea). (*B*) The angle of the pressure–pressure (P–P) curve is defined as the angle between the peak inspiratory and expiratory pressure points and the baseline of the angle. The P–P curves are linear and the angle of the P–P curve is close to 45°.

expiratory phases ($P = 0.653$). For patients with variable stenosis, the P–P curve appeared loop-shaped with a significant change in the angle of the P–P curve between inspiratory and expiratory phases ($P = 0.039$). For variable extrathoracic stenosis, the angle of the P–P curve during inspiration was smaller than during expiration. On the other hand, for variable intrathoracic stenosis, the angle of the P–P curve during expiration was smaller than during inspiration.

In a patient with fixed extrathoracic stenosis due to exuberant granulation tissue, multidetector computed tomography (MDCT) showed a weblike stenosis at the endotracheal tube cuff site (Figure 5A). Endobronchial ultrasonography (EBUS) revealed no cartilaginous abnormalities. Before balloon dilation, a considerable pressure difference between the upper trachea and carina was noted (Figure 5C). After resection, using the tip of a rigid bronchoscope and balloon dilation, MDCT showed restored patency of the trachea (Figure 5B), and the pressure difference disappeared (Figure 5D). Before dilation the P–P curve was linear, and the angle of the P–P curve was small during inspiration and expiration (Figure 5E). After dilation, the angle of the P–P curve increased from 0.5 to 38.2° (Figure 5E) and the MMRC Scale grade decreased from 2 to 0.

In a patient with variable extrathoracic stenosis due to esophageal cancer, MDCT showed dynamic airway collapse caused by excessive bulging of the left airway wall covered with a titanium mesh after tracheoplasty (Figure 5F). EBUS showed the cartilage layer was absent between the 7 and 10 o'clock positions. Before stenting, there was a considerable pressure difference between the upper trachea and carina (Figure 5H). After implantation of a self-expandable metallic stent, bronchoscopy confirmed that the trachea was patent and that the pressure difference disappeared (Figures 5G and 5I). Before stenting, the angle of the P–P curve during inspiration was smaller than during expiration, and the P–P curve appeared loop-shaped during the inspiratory phase (Figure 5J). After stenting, the angle of the P–P curve increased from 14.7 to 43.8° with a linear shape (Figure 5J), and the MMRC Scale grade decreased from 4 to 0.

In a patient with fixed intrathoracic stenosis due to choriocarcinoma, MDCT showed an extrinsic compression at the metastatic lymph nodes (Figure 6A). Before stenting, there was a considerable pressure difference between the upper trachea and carina (Figure 6C). After implantation of a self-expandable metallic stent, the trachea was clearly patent (Figure 6B) and the pressure difference disappeared (Figure 6D). Before stenting, the P–P curve was linear and the angle of the P–P curve was small during inspiration and expiration (Figure 6E). After stenting, the angle of the P–P curve increased from 1.7 to 40.6° (Figure 6E), and the MMRC Scale grade decreased from 2 to 0.

In a patient with variable intrathoracic stenosis due to colon cancer, MDCT showed compression from an extraluminal tumor on the right side (Figure 6F). EBUS showed that the cartilage layer was involved and interrupted around the tumor. Before stenting, a considerable pressure difference between the upper trachea and carina was noted (Figure 6H). After implantation of a self-expandable metallic stent, the trachea was patent (Figure 6G) and the pressure difference decreased (Figure 6I). Before stenting, the angle of the P–P curve during expiration was smaller than on inspiration and appeared loop-shaped (Figure 6J).

TABLE 4. DIAGNOSIS, CLASSIFICATION, AND NUMBER OF TRACHEAL OBSTRUCTION CASES

	Malignant			Benign	
Diagnosis	Endoluminal	Extrinsic	Mixed	Granulation	Malacia
Lung cancer		2	8		
Esophageal cancer		3	4		1
Thyroid cancer		1			
Colon cancer			1		
Laryngeal cancer		1			
Choriocarcinoma			1		
Adenoid cystic carcinoma	1		1		
Thymoma			1		
Tracheal tuberculosis				1	1
Postintubation tracheal stenosis				3	
Total	1	7	16	4	2
(Fixed/variable)	(0/1)	(2/5)	(13/3)	(3/1)	(0/2)

TABLE 5. DYSPNEA SCORE, PULMONARY FUNCTION TESTS, DEGREE OF OBSTRUCTION, PRESSURE DIFFERENCE, AND ANGLE OF PRESSURE–PRESSURE CURVE IN PATIENTS WITH TRACHEAL OBSTRUCTION BEFORE AND AFTER INTERVENTIONAL BRONCHOSCOPY

	Before	After	Responders
MMRC Scale	2.9 ± 1.0	0.9 ± 1.1*	21/30 (70%)†
VC, L	2.7 ± 1.1	2.9 ± 1.1	
VC, % predicted	83.3 ± 28.3	90.8 ± 28.0	
FVC, L	2.6 ± 1.1	2.9 ± 1.1‡	13/26 (50.0%)§
FEV_1, L	1.2 ± 0.6	2.0 ± 0.8*	21/26 (80.8%)‖
FEV_1, % predicted	48.7 ± 21.1	79.5 ± 27.2*	
FEV_1/FVC, %	48.1 ± 21.3	70.3 ± 20.0*	
PEF, L/s	2.1 ± 0.9	4.5 ± 1.8*	
Degree of tracheal obstruction, %	78.3 ± 9.2	44.7 ± 17.6*	
Pressure difference, cm H_2O	29.5 ± 25.1	2.3 ± 2.5*	
Angle of pressure–pressure curve, degrees	10.9 ± 12.8	36.4 ± 8.0*	

Definition of abbreviation: MMRC Scale = modified Medical Research Council Scale.

Continuous variables before and after intervention were tested by Wilcoxon signed-rank test. Values are represented as means ± standard deviation.

* $P < 0.0001$.

† ΔMMRC responder = improvement in MMRC Scale grade by 2 or more.

‡ $P < 0.05$.

§ ΔFVC responder = increase in posttreatment forced vital capacity of 12% or greater and an absolute change of 200 ml or more.

‖ ΔFEV_1 responder = increase in posttreatment FEV_1 of 12% or greater and an absolute change of 200 ml or more.

After stenting, the angle of the P–P curve increased from 0.6 to 27.9° and a linear shape was seen (Figure 6J). The MMRC Scale grade decreased from 2 to 0.

In a patient with variable intrathoracic stenosis due to tracheal tuberculosis, MDCT showed a severe saber-sheath type of tracheal malacia (Figure 7A). The cartilage was fractured at the 2 o'clock position and the submucosal layer of the membranous portion was thickened on EBUS. Before stenting, a pressure difference between the upper trachea and carina was noted (Figure 7B), and the angle of the P–P curve was small with a loop-shaped appearance (Figure 7C). The pressure difference during expiration was larger than during inspiration. The flow–volume curve showed a marked reduction of the expiratory flow with a plateau (Figure 7D), and negative expiratory pressure (NEP) measurements showed an expiratory flow limitation during tidal breathing (Figure 7E). After insertion of a silicone Y stent, tracheal patency was restored (Figure 7F). Pressure differences disappeared immediately after stent implantation (Figure 7G), and the angle of the P–P curve increased from 7.5 to 40.9° with a linear shape (Figure 7H). The flow–volume curve improved slightly but still showed flow limitation in the tidal range after stent placement (Figure 7I). The NEP measurements showed no expiratory flow limitation during tidal breathing after intervention (Figure 7J). The MMRC Scale grade decreased from 3 to 0.

This approach identified a need for additional treatment in three patients during interventional bronchoscopy. After initial stenting, bronchoscopy showed that the airway was patent; however, the angle of the P–P curve showed only a slight improvement. After subsequent treatments, the pressure difference and the angle of the P–P curve improved dramatically in these patients (Figure 8).

DISCUSSION

To our knowledge, this is the first prospective investigation demonstrating the usefulness of pressure differences and pressure–pressure (P–P) curves to measure lateral airway pressures (P_{lat}) on each side of a tracheal obstruction, using a dedicated double-lumen catheter during interventional bronchoscopy. Direct measurements of the pressure difference and the angle of the P–P curve are new assessment modalities for the success of interventional bronchoscopy in patients with tracheal obstruction. The degree of tracheal obstruction was significantly correlated with the pressure difference and the angle of the P–P curve. Furthermore, the MMRC Dyspnea Scale, the pressure difference, and the angle of the P–P curve showed significant changes beyond 50% obstruction. In this clinical study, preoperation measures by the baseline of the degree of tracheal obstruction could be used to predict the postoperation impact on

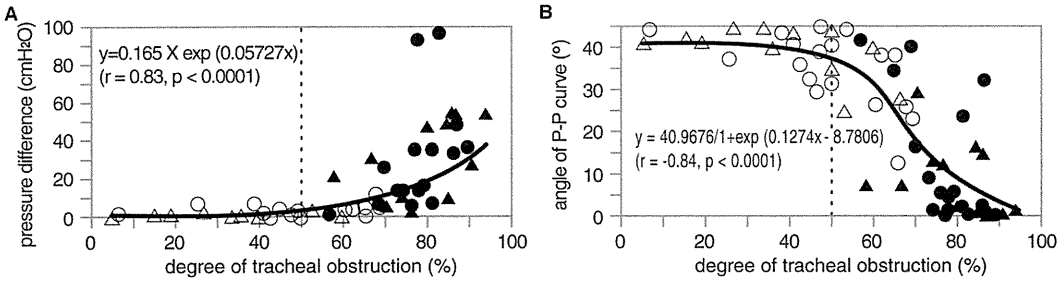

Figure 4. Scatter plot of pressure difference and the angle of the pressure–pressure (P–P) curve versus the degree of tracheal obstruction. *Solid circles*, before intervention; *open circles*, after intervention in cases with fixed stenosis. *Solid triangles*, before intervention; *open triangles*, after intervention in cases with variable stenosis. *Dotted line* shows the threshold for 50% tracheal obstruction. (*A*) The pressure difference and (*B*) the angle of the P–P curves are significantly correlated with the degree of tracheal obstruction ($r = 0.83$, $P < 0.0001$ and $r = -0.84$, $P < 0.0001$, respectively). (*A*) The pressure difference increased significantly above 50% obstruction and increased dramatically above 70% obstruction. (*B*) When the cross-sectional area was small, the angle of the P–P curve was close to 0°. After interventional bronchoscopy, the cross-sectional area increased and the angle of the P–P curve was close to 45°.

TABLE 6. RELATION BETWEEN BASELINE OF THE DEGREE OF TRACHEAL OBSTRUCTION AND THE CHANGE IN MODIFIED MEDICAL RESEARCH COUNCIL SCALE GRADE AFTER INTERVENTIONAL BRONCHOSCOPY

Degree of Tracheal Obstruction (%)	ΔMMRC*		
	≤1	≤2	Responders† (%)
50–60		2	10/17 (58.8%)
61–70	2	2	
71–80	5	6	
81–90	2	9	11/13 (84.6%)
91–100		2	

Definition of abbreviation: MMRC = modified Medical Research Council Scale.
* ΔMMRC = change in MMRC Scale grade.
† ΔMMRC responder = improvement in MMRC Scale grade by 2 or more.

TABLE 7. CORRELATIONS AMONG PRESSURE DIFFERENCE, ANGLE OF PRESSURE–PRESSURE CURVE, PULMONARY FUNCTION TESTS, AND DEGREE OF OBSTRUCTION IN TRACHEAL OBSTRUCTION CASES

	Pressure Difference		Angle of P–P Curve	
	r Value	*P* Value	*r* Value	*P* Value
MMRC Scale	0.63	<0.0001	−0.65	<0.0001
VC	−0.14	0.2478	0.09	0.4572
VC, % predicted	−0.26	0.0296	0.25	0.0375
FVC	−0.14	0.2523	0.09	0.4429
FEV_1	−0.45	<0.0001	0.44	0.0001
FEV_1, % predicted	−0.50	<0.0001	0.43	0.0002
FEV_1/FVC	−0.42	0.0002	0.46	<0.0001
PEF	−0.62	<0.0001	0.53	<0.0001
Degree of tracheal obstruction	0.83	<0.0001	−0.84	<0.0001

Definition of abbreviations: MMRC = modified Medical Research Council Scale; P–P = pressure–pressure.

Correlations among pressure difference, angle of the P–P curve, and cross-sectional area were evaluated using the Spearman correlation coefficient.

dyspnea. If the cross-sectional area (CSA) was small, then the angle was close to 0°; however, after intervention, the CSA significantly increased and the angle was close to 45°. In this clinical study, the pressure difference was used mainly to locate the site of maximal obstruction for the optimal positioning of the stent, and we used the angle of the P–P curve to assess the degree of tracheal obstruction quantitatively. The angle of the P–P curve was a visually simple way to assess the outcome of intervention in real time during bronchoscopy. In our experimental study, the angle of the P–P curve was unaffected by breathing maneuvers whereas the pressure difference was affected. Moreover, the shape of the P–P curve was useful in analyzing the nature of the stenosis. In fixed stenosis, the P–P curve was linear whereas in variable stenosis, the P–P curve was loop-shaped and a significant change was observed in the angle between inspiration and expiration. This bronchoscopic procedure made it possible to achieve complete remission in patients with tracheal obstruction. Furthermore, this approach provided useful information during the procedure to guide treatment decisions, such as additional stenting, balloon dilation, and laser ablation.

Measurement of Lateral Airway Pressure

Macklem and colleagues demonstrated that pressure drops down the bronchial tree by direct measurement of P_{lat}, esophageal pressure, and total flow during cine-bronchography (8). Healthy subjects have a relatively uniform pressure drop down the bronchial tree during expiration. In patients with airway stenosis, the major pressure drop occurs across the stenosis. Because P_{lat} may vary at different alveolar pressures and lung volumes, it is necessary to express P_{lat} as a percentage of alveolar pressure. We could detect the pressure difference between two sites (proximal and distal) of the stenotic segment and identify the site of maximal obstruction. A previous study reported that pressure differences changed dramatically from 70% tracheal obstruction (2). In cases with 50% tracheal obstruction, the highest velocities are in the jet, which is generated by glottic constriction. In cases with more than 70% tracheal obstruction, peak

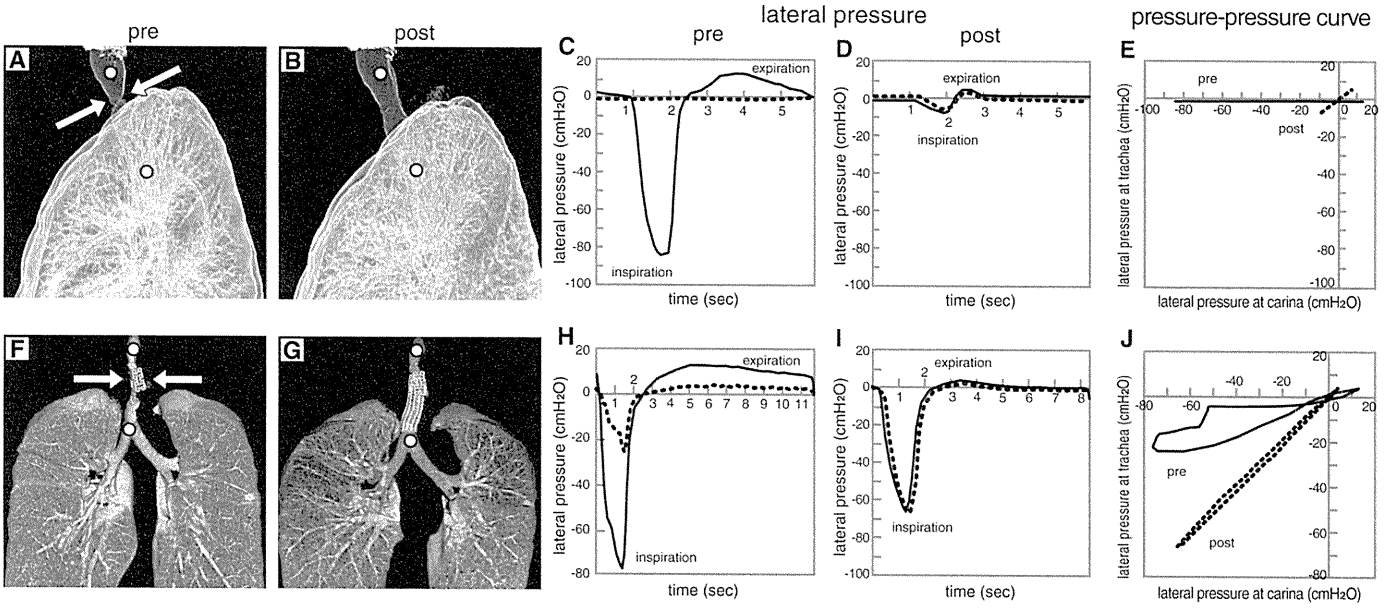

Figure 5. Patterns of lateral airway pressure (P_{lat}) measurement before and after interventional bronchoscopy for extrathoracic tracheal obstruction. (*A–E*) Fixed extrathoracic stenosis due to granulation tissue. (*F–J*) Variable extrathoracic stenosis due to esophageal cancer. *White arrows* indicate the area of stenosis. P_{lat} was measured simultaneously at the *white points* (upper trachea and carina). *Black lines* show P_{lat} at the carina and *dotted lines* indicate P_{lat} at the upper trachea. The pressure–pressure curve represented by the *black line* shows the result before the procedure and the *dotted line* shows the result after the procedure. See text for further explanation.

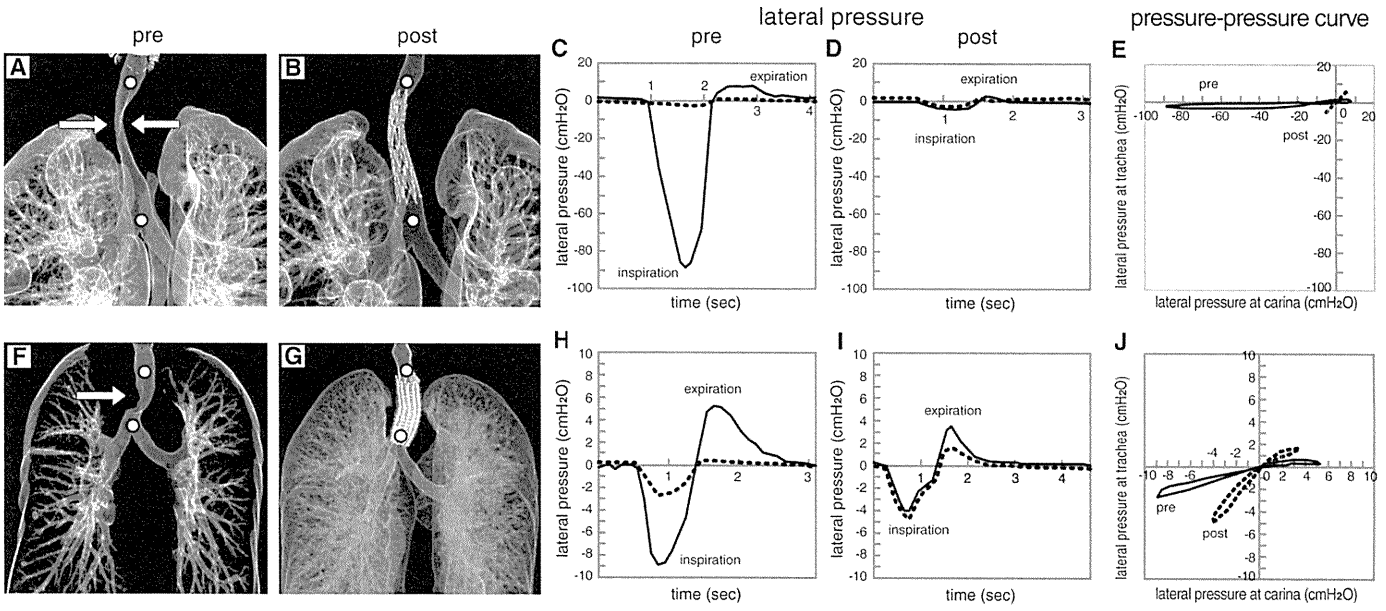

Figure 6. Patterns of lateral airway pressure (P_{lat}) measurement before and after interventional bronchoscopy for intrathoracic tracheal obstruction. (*A–E*) Fixed intrathoracic stenosis due to choriocarcinoma. (*F–J*) Variable intrathoracic stenosis due to colon cancer. *White arrows* indicate the area of stenosis. P_{lat} was measured simultaneously at the *white points* (upper trachea and carina). *Black lines* show P_{lat} at the carina and *dotted lines* indicate P_{lat} at the upper trachea. The pressure–pressure curve represented by the *black line* shows the result before the procedure and the *dotted line* shows the result after the procedure. See text for further explanation.

velocities are generated at the stenosis and exceed velocities in the glottic area. However, in the present study, we found that pressure differences significantly increased from 50% obstruction in the trachea after measuring P_{lat} at two points with a rigid bronchoscope. The contrast in pressure differences obtained in this study during intubation with a rigid bronchoscope, compared with those obtained in simulated models without intubation (2), might be attributed to the existence of glottis.

Wave-speed flow limitation during expiration is affected by the relationship between transmural pressure and the CSA of the airway (23, 24). When pleural pressure was measured with an esophageal balloon (25), insertion of the balloon could not be performed in patients with esophageal cancer. However, this new technique does not require an esophageal balloon and is simple, safe, and feasible to perform.

In extensive fixed tracheal stenosis, sometimes we can observe considerable dynamic stenosis in the airways below the obstruction. In our previous study (4), after stenting, the migration of the flow-limiting segment (FLS) to nonstented segments of the weakened airway resulted in its subsequent collapse.

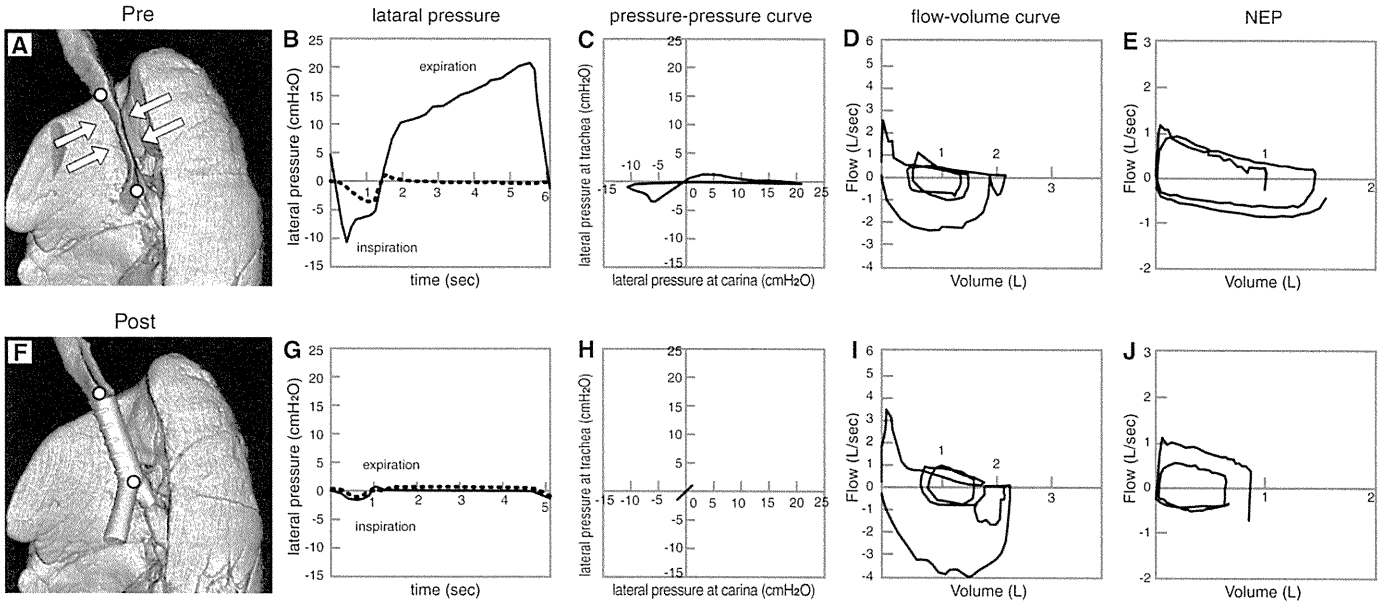

Figure 7. Lateral airway pressure (P_{lat}) measurements before and after interventional bronchoscopy with a silicone Y stent in tracheobronchial malacia due to tuberculosis (*A–E*, before; *F–J*, after). *White arrows* indicate the area of stenosis. P_{lat} was measured simultaneously at the *white points* (upper trachea and carina). (*B* and *G*) The *black line* shows P_{lat} at the carina and the *dotted line* indicates P_{lat} at the upper trachea. See text for further explanation. NEP = negative expiratory pressure.

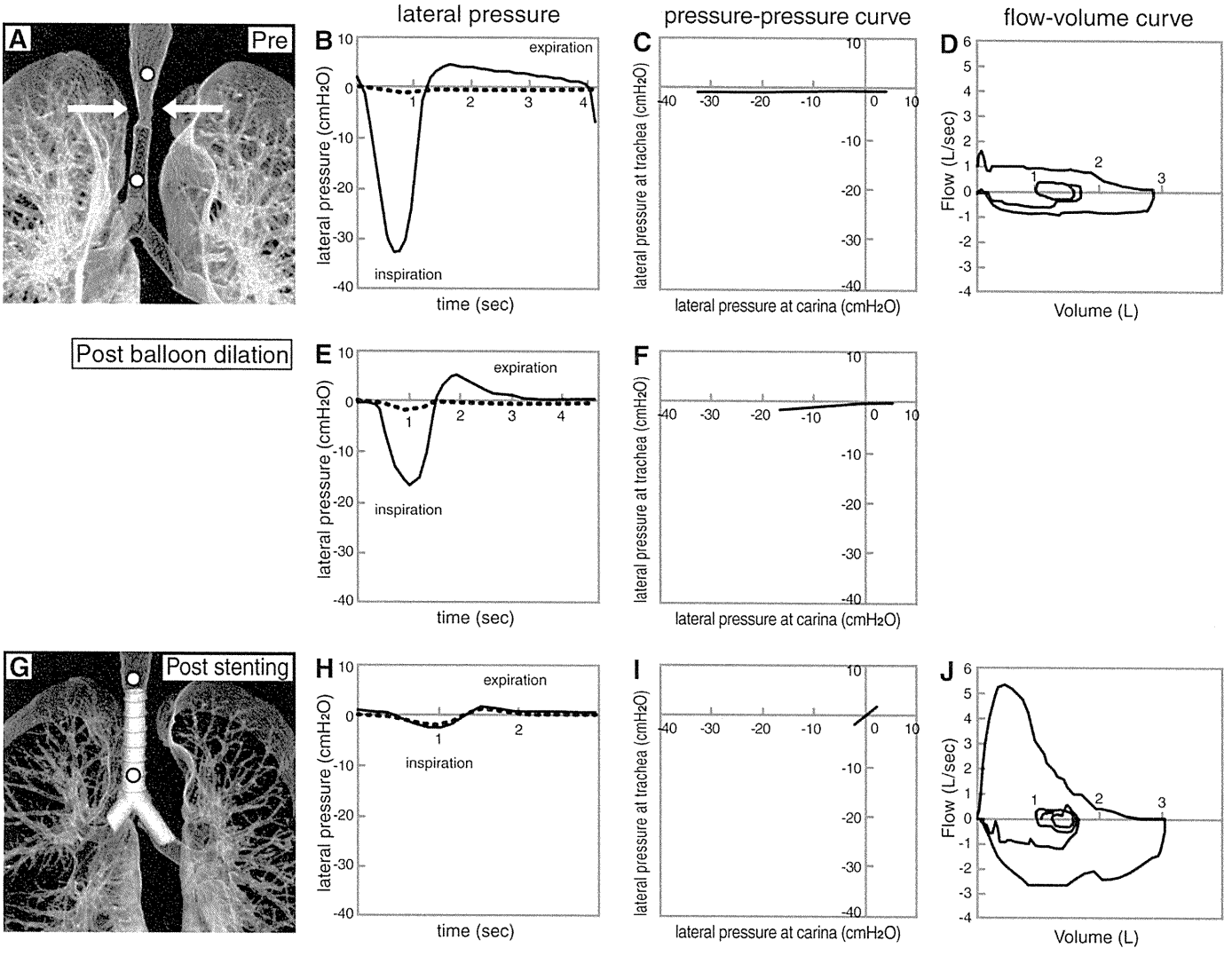

Figure 8. Lateral airway pressure (P_{lat}) measurements during interventional bronchoscopy with balloon dilation and silicone Y stent implantation in fixed intrathoracic stenosis due to tracheobronchial tuberculosis (*A–D*, before treatment; *E* and *F*, after balloon dilation; *G–J*, after stenting). *White arrows* indicate the area of stenosis. P_{lat} was measured simultaneously at the *white points* (upper trachea and carina). In (*B*), (*E*), and (*H*), the *black line* shows P_{lat} at the carina and the *dotted line* indicates P_{lat} at the upper trachea. After each treatment, the pressure difference and the angle of the P–P curve improved.

Additional stenting at the migrated FLS results in functional improvement in patients with extensive stenosis. In this study, by measuring P_{lat}, the precise site of maximal obstruction could be easily identified when additional dynamic collapse occurred on the distal side of the stenosis.

Assessment of the P–P Curve

Central airway stenosis can be divided into four major types: fixed, variable, extrathoracic, and intrathoracic stenosis. In fixed stenosis, the CSA at the site of the lesion does not change during the respiratory cycle. In variable stenosis, the configuration of the stenotic lesion changes between phases of respiration. Airway narrowing occurs during expiration in intrathoracic stenosis, whereas airway narrowing occurs during inspiration in extrathoracic stenosis. In variable extrathoracic stenosis, the angle of the P–P curve during inspiration is smaller than during expiration, and in variable intrathoracic stenosis, the angle of the P–P curve during expiration is smaller than during inspiration.

An extremely compliant central airway can collapse during quiet breathing with minimal transmural pressure (26). In weak tracheal cartilaginous structures, the negative transmural pressure gradient can cause increased airway collapsibility and narrowing. This increases airway resistance and airflow no longer increases with driving pressure. In this study, the P–P curve of a patient with tracheal malacia appeared as loop-shaped. P–P curves can be used to select the appropriate expansion force and elasticity of the stent.

Although bronchoscopic images showed that tracheal patency was restored after procedures, the angle of the P–P curve did not always improve. It is difficult to estimate the outcome of interventional procedures by bronchoscopy alone. We could identify whether the widening effect of the stent was sufficient and the stent length was long enough to fully cover the stenosis by calculating the angle of the P–P curve. Measuring P_{lat} can physiologically estimate the need for additional procedures and the desired outcome.

Author disclosures are available with the text of this article at www.atsjournals.org.

Acknowledgment: The authors thank Mr. Jason Tonge from St. Marianna University School of Medicine for reviewing the language of this manuscript. The authors also thank Dr. Shinobu Tatsunami of the Medical Statistics Department at St. Marianna University School of Medicine for valuable advice on the statistical analysis.

References

1. Seijo LM, Sterman DH. Interventional pulmonology. *N Engl J Med* 2001;344:740–749.
2. Brouns M, Jayaraju ST, Lacor C, Mey JD, Noppen M, Vincken W, Verbanck S. Tracheal stenosis: a flow dynamics study. *J Appl Physiol* 2007;102:1178–1184.
3. Miyazawa T, Yamakido M, Ikeda S, Furukawa K, Takiguchi Y, Tada H, Shirakusa T. Implantation of Ultraflex nitinol stents in malignant tracheobronchial stenoses. *Chest* 2000;118:959–965.
4. Miyazawa T, Miyazu Y, Iwamoto Y, Ishida A, Kanoh K, Sumiyoshi H, Doi M, Kurimoto N. Stenting at the flow-limiting segment in tracheobronchial stenosis due to lung cancer. *Am J Respir Crit Care Med* 2004;169:1096–1102.
5. Mink S, Ziesmann M, Wood JDH. Mechanisms of increased maximum expiratory flow during HeO_2 breathing in dogs. *J Appl Physiol* 1979; 47:490–502.
6. Smaldone GC, Itoh H, Swift DL, Wagner HN. Effect of flow-limiting segments and cough on particle deposition and mucociliary clearance in the lung. *Am Rev Respir Dis* 1979;120:747–758.
7. Pedersen OF, Thiessen B, Lyager S. Airway compliance and flow limitation during forced expiration in dogs. *J Appl Physiol* 1982;52:357–369.
8. Macklem PT, Fraser RG, Bates DV. Bronchial pressures and dimensions in health and obstructive airway disease. *J Appl Physiol* 1963;18: 699–706.
9. Smaldone GC, Smith PL. Location of flow-limiting segments via airway catheters near residual volume in humans. *J Appl Physiol* 1985;59: 502–508.
10. Pedersen OF, Brackel HJ, Bogaard JM, Kerrebijn KF. Wave-speed–determined flow limitation at peak flow in normal and asthmatic subjects. *J Appl Physiol* 1997;83:1721–1732.
11. Pedersen OF, Ingram RH Jr. Configuration of maximum expiratory flow–volume curve: model experiments with physiological implications. *J Appl Physiol* 1985;58:1305–1313.
12. Ohya N, Huang J, Fukunaga T, Toga H. Airway pressure–volume curve estimated by flow interruption during forced expiration. *J Appl Physiol* 1989;67:2631–2638.
13. Pedersen OF; Peak Flow Working Group. Physiological determinants of peak expiratory flow. *Eur Respir J* 1997;10:11–16.
14. Aljuri N, Freitag L, Vegegas JG. Modeling expiratory flow from excised tracheal tube law. *J Appl Physiol* 1999;87:1973–1980.
15. Miller RD, Hyatt RE. Evaluation of obstructing lesions of the trachea and larynx by flow–volume loops. *Am Rev Respir Dis* 1973;108:475–481.
16. Nishine H, Hiramoto T, Kida H, Ishikawa F, Nakamura M, Saji J, Oshige M, Ishida A, Nobuyama S, Hoshino M, *et al.* Airway catheterization in the assessment of tracheal stenosis during interventional bronchoscopy [abstract]. *Eur Respir J* 2008;32:249S.
17. Nishine H, Hiramoto T, Kida H, Inoue T, Mineshita M, Miyazawa T. Assessment of central airway stenosis using intra-airway pressure [abstract]. *Am J Respir Crit Care Med* 2009;179:A6164.
18. Matsuoka S, Kurihara Y, Yagihashi K, Hoshino M, Nakajima Y. Airway dimensions at inspiratory and expiratory multisection CT in chronic obstructive pulmonary disease: correlation with airflow limitation. *Radiology* 2008;248:1042–1049.
19. Matsuoka S, Kurihara Y, Yagihashi K, Hoshino M, Watanabe N, Nakajima Y. Quantitative assessment of air trapping in chronic obstructive pulmonary disease using inspiratory and expiratory volumetric MDCT. *AJR Am J Roentgenol* 2008;190:762–769.
20. Nuutinen J. Acquired tracheobronchomalacia: a bronchological follow-up study. *Ann Clin Res* 1977;9:359–364.
21. Baroni RH, Feller-Kopman D, Nishino M, Hatabu H, Lorong SH, Ernst A, Boiselle PM. Tracheobronchomalacia: comparison between end-expiratory and dynamic expiratory CT for evaluation of central airway collapse. *Radiology* 2005;235:635–641.
22. Carden KA, Boiselle PM, Waltz DA, Ernst A. Tracheomalacia and tracheobronchomalacia in children and adults. *Chest* 2005;127:984–1005.
23. Dawson SV, Elliot EA. Wave-speed limitation on expiratory flow a unifying concept. *J Appl Physiol* 1977;43:498–515.
24. Mead J. Expiratory flow limitation: a physiologist's point of view. *Fed Proc* 1980;39:2771–2775.
25. Milic-Emili J, Mead J, Turner JM, Glauser EM. Improved technique for estimating pleural pressure from esophageal balloons. *J Appl Physiol* 1964;19:207–211.
26. Teng Z, Ochoa I, Li Z, Liao Z, Lin Y, Doblare M. Study on tracheal collapsibility, compliance, and stress by considering nonlinear mechanical property of cartilage. *Ann Biomed Eng* 2009;37:2380–2389.

原　著

聖マリアンナ医科大学雑誌
Vol. 39, pp. 113-121, 2011

中枢気道狭窄の評価における impulse oscillation system (IOS) の有用性の研究

半田　寛　峯下　昌道　古屋　直樹　木田　博隆
西根　広樹　井上　健男　延山　誠一　宮澤　輝臣

（受付：平成23年 8 月19日）

抄　録

背景: 中枢気道狭窄の評価は気管支鏡，胸部 CT，スパイロメトリーなどで行われているが，重篤な病態で緊急に処置を要する症例も多く，侵襲の低い検査が望まれる。Impulse oscillation system (IOS) は安静呼吸で呼吸抵抗，呼吸リアクタンスを評価できる検査である。今回，IOS による中枢気道狭窄病変の評価が可能であるかを検討した。

方法: 2008年4月から2010年2月までに当院を受診した気管狭窄症例 (17症例) 及び主気管支狭窄 (13例) においてスパイロメトリーと IOS との相関関係を検討した。さらに悪性腫瘍による気管狭窄症例において CT で測定した最狭部の面積と，スパイロメトリーと IOS の各指標との相関を検討した。

結果: 気管支狭窄では呼吸抵抗とリアクタンスの両方ともスパイロメトリーとの有意な強い相関関係がみられた。一方，気管狭窄ではスパイロメトリーとの相関はみられなかった。悪性腫瘍による気管狭窄を呈した13例の検討では，最狭窄部の断面積との相関はスパイロメトリーでは PEF ($r=0.626$, $p=0.022$)，IOS では R5 ($r=-0.819$, $p<0.001$)，R20 ($r=-0.603$, $p=0.290$)，X20 ($r=0.597$, $p=0.031$) で認められた。特に R5 で最も良い相関が得られた。

結論: IOS は悪性腫瘍による気管狭窄症例でスパイロメトリーと比較し狭窄病変の程度をより反映できると考えられた。一方，気管支狭窄ではスパイロメトリーと同様に健側肺の状況を反映すると考えられ狭窄部の評価は難しいと考えられた。努力非依存性である IOS は気管狭窄の生理学的評価に有用と考えられる。

牽引用語

impulse oscillation system, スパイロメトリー，呼吸抵抗，リアクタンス

緒　言

中枢気道狭窄の部位を評価する画像的な方法として胸部 CT と気管支鏡が主に用いられるが，生理学的な指標として呼吸機能検査，特にフローボリューム曲線が狭窄部位の推定に応用されている[1]。しかし，フローボリューム曲線を得るためには強制呼吸が必要であるため，呼吸困難が強い場合や精神疾患を有するような患者では正確な評価が困難である。

Impulse oscillation system (IOS) は forced oscillation technique (FOT) の一つでありラウドスピーカーから0から 100Hz の周波数成分を含んだインパルス信号を放出させ，安静呼吸下の口腔の流速と圧力を計測した結果をフーリエ変換し呼吸インピーダンスを解析することができる呼吸抵抗測定装置である[2-4]。呼吸インピーダンスは呼吸抵抗とリアクタンスに分けることができ，気道狭窄の程度や肺の弾性コンプライアンスを食道バルーンやガスを用いな

聖マリアンナ医科大学　内科学(呼吸器・感染症内科)

Table 1. Characteristics of Patients.

	Tracheal (n=17)	Bronchial (n=13)
Male/Female	13/4	6/7
Age (years)	62±13	56±16
Body weight (kg)	53.7±13.1	59.6±11.7
Height (cm)	160.7±7.6	161.9±6.58
Body surface area (m^2)	1.54±0.18	1.62±0.13
Smoking (Pack-years)	23.9±20.1	30.7±26.6
MMRC *	3.0±1.0	2.1±1.0
Benign disease		
Granuloma	1	0
Relapsing Polychondritis	2	0
Post Tuberculosis	1	2
Wegener granulomatosis	0	1
Malignant disease		
Lung Cancer	4	7
Esophageal Cancer	6	1
Bronchial gland carcinoma	3	1
Carcinoid tumour	0	1

MMRC: modified medical research council, *P<0.05 tracheal stenosis vs bronchial stenosis

いで安全に評価できる。一般的に周波数の低いインパルス波は末梢まで届くと考えられており，5Hzでの粘性抵抗(Respiratory resistance at 5Hz: R5)は全肺気道成分を示し，20Hzでの粘性抵抗(Respiratory resistance at 20Hz: R20)は中枢気道成分を示しR5-R20は末梢気道成分を示すと解釈されている。また，リアクタンスは弾性抵抗と慣性抵抗の二つで成り立つが，5Hzのリアクタンス(reactance at 5 Hz: X5)は慣性抵抗を無視できるため末梢容量性リアクタンスとして末梢気道での弾性抵抗を示すとされ，20Hzのリアクタンス(reactance at 20Hz: X20)および共振周波数(resonant frequency: Fres)は肺の収縮に抵抗がある場合に高値になるため中枢気道狭窄がある場合は高値になる。IOSは小児を含む気管支喘息や慢性閉塞性肺疾患(chronic obstructive pulmonary disease: COPD)の評価に用いられている。最近，中枢気道病変においてもIOSは応用されており，神経疾患に合併した気管狭窄の検討[5]や，気管狭窄の程度と気道抵抗との相関に関する報告[6]もある。努力非依存性のIOSは呼吸困難を伴う気道狭窄症例の生理学的評価として有用であると考え，本研究では気管狭窄及び気管支狭窄症例において従来の標準的な呼吸機能検査であるスパイロメトリーとIOSの各指標間の相関を解析した。また気管狭窄症例においては呼吸による気道径の変動が比較的少ない悪性気道狭窄症例について，CTを用いて計測した最狭窄部の断面積と，スパイロメトリーおよびIOSの各指標の相関も検討した。

方　法

2008年4月から2010年2月までに胸部CTもしくは気管支鏡で診断された気道狭窄症例の内，スパイロメトリーとIOSを行った17名の気管狭窄症例と13名の気管支狭窄症例を対象としレトロスペクティブに解析を行った。なお本研究は聖マリアンナ医科大学の生命倫理委員会で承認されている(第1519号)。なお気道ステント留置後，気管切開後，及び片肺全摘を行った患者は除外とした。IOSは

マスタースクリーン IOS (CareFusion, Hochberg, Germany) を用いて，欧州呼吸器学会のプロトコールに準じて測定し[7]，R5, R20, X5, X20, および Fres を評価項目として使用した。スパイロメトリーは FUDAC-77 (Fukuda Electronics, Tokyo, Japan) を用いて IOS を測定した後に行い，努力肺活量 (FVC: forced vital capacity)，一秒量 (FEV 1.0: forced expiratory volume at 1 second)，最大呼気流速 (PEF: peak expiratory flow)，50%排気量位における最大努力呼気流速 (FEF50: forced expiratory flow after 50%)，25%排気量位における最大努力呼気流速 (FEF25: forced expiratory flow after 25%) を評価項目として使用した。また，悪性腫瘍による気管狭窄症例 13 例を Ziostation™ (Ziosoft, Tokyo, Japan) を使用し胸部 CT で最狭窄部の断面積を測定しスパイロメトリーと IOS との相関関係を調べた。CT (Aquilion-64; Toshiba Medical, Tokyo, Japan) の撮影条件は松岡ら[8]の方法を用い，phantom study にてその整合性は示されている。今回の検討では，画像上呼気に伴う動的な気道径で狭窄の性状の変動が著明な良性疾患を除外して検討を行った。統計学的解析は JMP5.0 (SAS Institute, Cary, NC, USA) を用いて行った。IOS とスパイロメトリーの比較を Mann-Whitney U 試験を用い，相関関係を Spearman's correlation を用いて行い，$p<0.05$ を有意差ありとした。

結　果

気管狭窄と気管支狭窄の症例の内訳 (**Table 1**) では，気管狭窄症例は主気管支狭窄症例に比べ呼吸困難の指標である modified medical research council (MMRC) スコアが有意に高く，高齢かつ女性が多い傾向にあったが，身長，体重や body surface area (BSA) に差はみられなかった。喫煙は主気管支狭窄症例の方が多かった。気管狭窄では良性疾患として軟化症を発症した再発性多発軟骨炎を 2 例，気管気管支結核後遺症による気管軟化症を 1 例，原因不明の肉芽腫狭窄を 1 例でありすべての症例で呼気に伴う気道径の変動があり呼気に気道閉塞を起こしていた。悪性疾患としては肺癌 4 例，食道癌 6

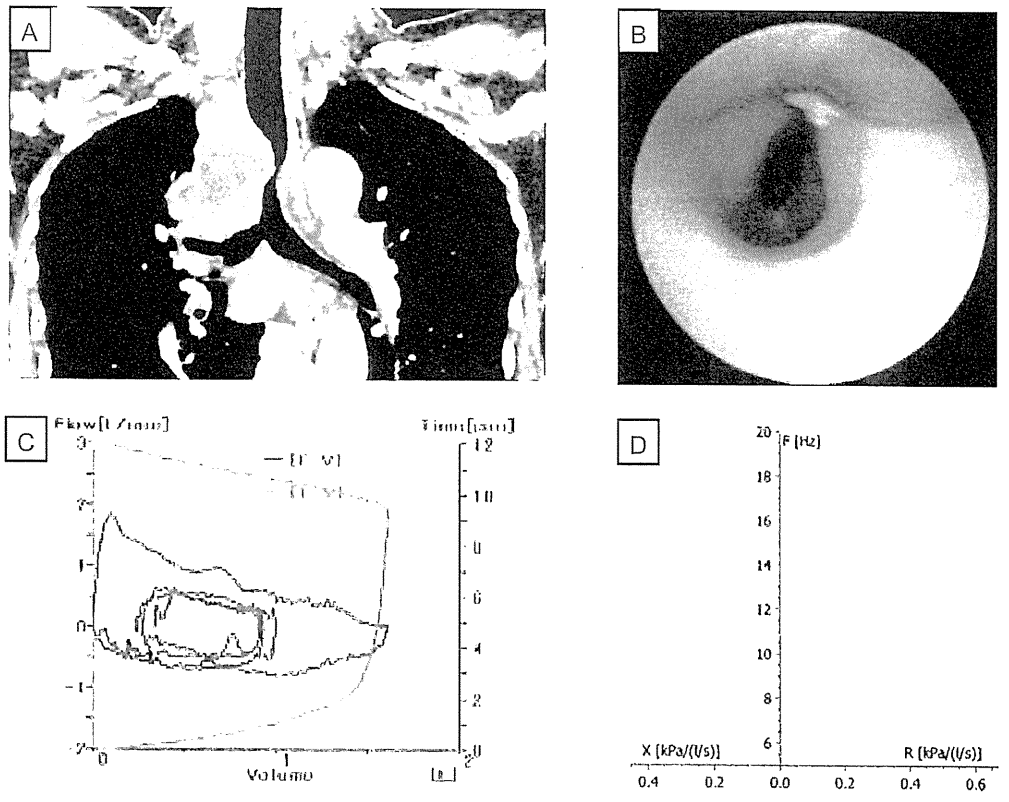

Fig. 1. CT and bronchoscopic findings show the tracheal narrowing due to mediastinal lymphadenopathy (**A, B**). Flow-volume curve shows a marked reduction of the expiratory flow with a plateau (**C**). IOS shows the increase inrespiratory resistance and the decrease in respiratory reactance (**D**).

Table 2. Pulmonary Function Tests in Tracheal and Bronchial Stenosis.

	Tracheal (n=17)	Bronchial (n=13)
Spirometry		
FVC (L)	2.35±0.63	2.33±0.83
$FEV_{1.0}$ (L)	1.08±0.66	1.34±0.42
PEF (L/s)*	2.15±1.05	3.59±1.52
FEF50	1.02±0.90	1.11±0.56
FEF25	0.49±0.37	0.41±0.26
IOS		
R5	0.60±0.24	0.52±0.23
(IN,EX)	(0.56±0.19,0.64±0.41)	(0.47±0.20,0,55±0.24)
R20	0.36±0.09	0.35±0.09
(IN,EX)	(0.33±0.13,0.34±0.08)	(0.33±0.09,0.36±0.10)
R5-R20	0.24±0.19	0.17±0.17
(IN,EX)	(0.22±0.16,0.25±0.24)	(0.15±0.13,0.17±0.18)
X5	-0.26±0.17	-0.26±0.16
(IN,EX)	(-0.24±0.14,-0.30±0.26)	(-0.23±0.10,-0.28±0.24)
X20	-0.05±0.08	-0.04±0.09
(IN,EX)	(-0.06±0.07,-0.04±0.10)	(-0.02±0.07,-0.04±0.10)
Fres	22.73±6.94	21.36±6.72
(IN,EX)	(23.13±6.08,22.65±7.53)	(21.20±6.70,21.31±6.78)

All parameters are mean values ±SD, *P<0.05

FVC: forced vital capacity, FEV1.0: forced expiratory volume at 1 second, PEF: peak expiratory flow, FEF50: forced expiratory flow after 50%, FEF25: forced expiratory flow after 25%, R5: respiratory resistance at 5Hz,R20: respiratory resistance at 20Hz, X5: reactance at 5Hz, X20: reactance at 20Hz, Fres: resonant frequency,IN: inspiration, EX: expiration

例，気管支腺癌3例で肺癌と食道癌は縦隔リンパ節腫大や直接浸潤による狭窄であり，気管支腺癌はポリープ状に内腔に突出した病変であった。主気管支狭窄症例では良性疾患では左側の気管支結核後遺症による狭窄が2例，Wegener 肉芽腫による両側の主気管支狭窄が1例を含み，悪性疾患では肺癌および食道癌による縦隔リンパ節浸潤による両側主気管支狭窄が3例，肺癌および気管支腺癌の原発巣が直接浸潤し片側の主気管支狭窄を起こした5例，左側の主気管支内腔にポリープ状に突出したカルチノイドが1例であった。気管狭窄はすべて胸腔内気管狭窄であり，気管支狭窄は片側が9例，両側が4例であった。

日本の健常な成人男性の予測式と再現性についての報告によると 166 人の健常な非喫煙者の R5 は 0.28±0.07kPa(l/s)，R20 は 0.24±0.06kPa(l/s)，X5 は−0.11kPa(l/s) であった[9]。気管狭窄と気管支狭窄症例のスパイロメトリーと IOS の所見では，気管狭窄と気管支狭窄症例の比較に於いて，PEF が気管狭窄症例で有意に低い他はスパイロメトリー，IOS 共に2群間で有意差はみられなかった (**Table 2**)。気管狭窄 17 例では IOS のパラメーターとスパイロメトリーと有意な相関関係はみられたのは吸気 X20 のみであり (**Table 3**)，気管支狭窄 13 例では IOS とスパイロメトリーとの相関は気流制限の指標である FEV1.0 と PEF が呼吸抵抗とリアクタン

Table 3. Correlation between Spirometric and IOS Measurements in Tracheal Stenosis.

Tracheal (n-17)	FVC r value	FEV1.0 r value	PEF r value	FEF50 r value	FEF25 r value
R5 (IN,EX)	-0.01 (-0.05,-0.07)	-0.42 (-0.38,-0.32)	-0.50 (-0.41,-0.47)	-0.48 (-0.44,-0.39)	-0.46 (-0.36,-0.38)
R20 (IN,EX)	0.12 (0.09,0.15)	-0.12 (-0.11,-0.01)	-0.36 (-0.32,-0.39)	-0.18 (-0.22,-0.39)	-0.23 (-0.27,-0.37)
R5-R20 (IN,EX)	0.02 (-0.01,0.08)	-0.35 (-0.39,-0.20)	-0.27 (-0.26,-0.28)	-0.40 (-0.39,-0.26)	-0.37 (-0.42,-0.25)
X5 (IN,EX)	0.28 (0.36,0.26)	0.20 (0.10,0.19)	-0.02 (-0.18,-0.40)	0.18 (0.02,0.25)	0.14 (-0.01,0.23)
X20 (IN,EX)	0.01 (0.02,-0.03)	0.24 (0.38,0.40)	0.41 (0.54*,0.40)	0.42 (0.54*,0.38)	0.40 (0.46,0.33)
Fres (IN,EX)	0.05 (-0.04,0.09)	-0.22 (-0.21,-0.13)	-0.26 (-0.23,-0.31)	-0.43 (-0.42,-0.35)	-0.31 (-0.22,-0.33)

*$P<0.05$

Table 4. Correlation between Spirometric and IOS Measurements in Bronchial Stenosis.

Bronchial (n=13)	FVC r value	FEV1.0 r value	PEF r value	FEF50 r value	FEF25 r value
R5 (IN,EX)	-0.66* (-0.63*,-0.75**)	-0.70** (-0.59,-0.73**)	-0.74** (-0.72**,-0.75**)	-0.70** (-0.60*,-0.70**)	-0.59* (-0.48,-0.57*)
R20 (IN,EX)	-0.46 (-0.44,-0.43)	-0.68* (-0.67*,-0.69**)	-0.72** (-0.74**,-0.72**)	-0.42 (-0.45,-0.42)	-0.32 (-0.36,-0.32)
R5-R20 (IN,EX)	-0.70** (-0.72**,-0.68**)	-0.62* (-0.57*,-0.55)	-0.79** (-0.56*,-0.82**)	-0.80** (-0.68*,-0.75**)	-0.63* (-0.61*,-0.62*)
X5 (IN,EX)	0.56* (0.25,0.57*)	0.49 (0.13,0.55)	0.63* (0.33,0.55)	0.60* (0.29,0.62*)	0.38 (0.24,0.44)
X20 (IN,EX)	0.66* (0.61*,0.70**)	0.57* (0.50,0.55)	0.74** (0.75**,0.71**)	0.73** (0.62*,0.69**)	0.60* (0.55,0.56*)
Fres (IN,EX)	-0.42 (-0.41,-0.52)	-0.47 (-0.45,-0.47)	-0.65* (-0.70**,-0.64*)	-0.68* (-0.69**,-0.69**)	-0.69** (-0.50,-0.50)

*$P<0.05$, **$P<0.01$

スともに有意な相関がみられた (**Table 4**)。

気管狭窄症例では，肺癌による縦隔リンパ節腫大により気管の圧排狭窄を来し (**Fig 1A**)，気管支鏡で高度の気管狭窄を認め (**Fig 1B**)，呼吸困難スコアMMRC3と高値であった。フローボリュームカーブでは高度の呼気気流制限がみられ (**Fig 1C**)，IOSでは低周波数領域を中心とした著明な呼吸抵抗の上昇とリアクタンスの低下がみられた (**Fig 1D**)。主気管支狭窄では，気管支結核後遺症による左主気管支狭窄を来たし (**Fig 2A**)，気管支鏡では線維化を伴った瘢痕狭窄を認め (**Fig 2B**)，MMRCは2と軽度であった。スパイロメトリーでは呼気気流制限を認めており (**Fig 2C**)，IOSでも呼吸抵抗の軽度上昇を認めたがリアクタンスの低下はみられなかった (**Fig 2 D**)。

悪性腫瘍による気管狭窄13例のCTでの最狭窄部の断面積とスパイロメトリー，IOSとの相関関係を解析した結果，スパイロメトリーではPEF ($r=0.626$, $p=0.022$) のみに有意な相関が得られたが，IOSではR5 ($r=-0.819$, $p<0.001$)，R20 ($r=-$